Energy & Environmental Science

COMMUNICATION

View Article Online
View Journal | View Issue

Cite this: *Energy Environ. Sci.*, 2016, **9**, 3650

Received 12th October 2016,
Accepted 28th October 2016

DOI: 10.1039/c6ee02980a

www.rsc.org/ees

Is Cu a stable electrode material in hybrid perovskite solar cells for a 30-year lifetime?†

Jingjing Zhao,[a] Xiaopeng Zheng,[a] Yehao Deng,[a] Tao Li,[b] Yuchuan Shao,[a] Alexei Gruverman,[b] Jeffrey Shield[a] and Jinsong Huang*[a]

One grand challenge for long-lived perovskite solar cells is that the common electrode materials in solar cells, such as silver and aluminum or even gold, strongly react with hybrid perovskites. Here we report the evaluation of the potential of copper (Cu) as the electrode material in perovskite solar cells for long-term stability. In encapsulated devices which limit exposure to oxygen and moisture, Cu in direct contact with $CH_3NH_3PbI_3$ showed no reaction at laboratory time scales, and is predicted to be stable for almost 170 years at room temperature and over 22 years at the nominal operating cell temperature of 40 °C. No diffusion of Cu into $CH_3NH_3PbI_3$ has been observed after thermal annealing for over 100 hours at 80 °C, nor does Cu cause charge trap states in direct contact with $CH_3NH_3PbI_3$ after long-term thermal annealing or illumination. High performance devices with efficiency above 20% with a Cu electrode retain 98% of the initial efficiency after 816 hours storage in an ambient environment without encapsulation. The results indicate Cu is a promising low-cost electrode material for perovskite solar cells for long-term operation.

Broader context

Perovskite solar cells are arising as strong candidates for next generation of renewable and clean energy conversion due to the very high efficiency achieved, low material and fabrication cost, and scalable manufacture capability. However the instability of perovskite materials remain a huge hurdle to be overcome before the commercialization of this technology. Among various instability issue associated with perovskite solar cells, one grand challenge which has rarely been addressed is the corrosion of many common metal electrode materials by perovskite, such as silver, aluminum or even gold. A diffusion barrier layer is generally inserted between the metal electrodes and perovskite layer to extend the short-term lifetime, which however doesn't solve the long-term stability problem. Here we reported the potential of low cost metal copper (Cu) as the electrode material for long-lived perovskite solar cells that potentially allows the stable operation of perovskite solar cells for over 20 years at nominal operation temperature even with the direct contact of Cu with perovskite. The commercial availability of Cu ink or Cu paste also allows the scalable manufacturing of perovskite solar cells with Cu electrodes.

Introduction

Organic–inorganic halide perovskite (OIHP) solar cells have been attracting increased attention in both academia and industry for their applications for the next generation of renewable energy converters with rapid energy payback time.[1] Their prospects to compete with other types of thin film solar cells have been rising due to the rapid progress in increasing efficiencies for both small and large area devices, as well as those fabricated with scalable methods.[2–19] The power conversion efficiency (PCE) has been increased to over 22% for small area devices,[20] and close to 20% for 1 cm^2 size devices.[21] However, the broadly observed poor stability of perovskite solar cells has remained a significant challenge that hinders the commercialization of OIHP solar cells.[22–24] Among all the factors that cause the instability of perovskite solar cells, the reaction between common electrode materials and the OIHP creates significant degradation and must be overcome for effective commercialization. The common metal electrodes, such as silver (Ag) and aluminum (Al), corrode when in contact with the hybrid perovskite.[25,26] Even noble metals, such as expensive gold (Au), were found to react with hybrid perovskite in short-term studies.[27] In order to fabricate a stable perovskite solar cells, diffusion barrier layer(s) was (were) often needed to be inserted to separate the metal electrodes and the perovskite layer.[28–32] These buffer layers may prevent the contact between the perovskite and metals over short time frames, but cannot solve the long-term stability issue, as materials tend to diffuse through the buffer layers after several months or years of operation under illumination or thermal cycles. The diffusion of Au across the thick hole transport layer was reported recently, which resulted in the degradation of the devices in several hours.[33]

[a] *Department of Mechanical and Materials Engineering and Nebraska Center for Materials and Nanoscience, University of Nebraska-Lincoln, Lincoln, NE 68588-0656, USA. E-mail: jhuang2@unl.edu*
[b] *Department of Physics and Astronomy, University of Nebraska-Lincoln, Lincoln, Nebraska 68588, USA*

† Electronic supplementary information (ESI) available. See DOI: 10.1039/c6ee02980a

The corrosion of Ag and Al electrodes by OIHPs has been generally ascribed to the chemical reaction of the metal electrodes with the decomposition products of perovskites (eqn (1)).[25,26] For example, HI from the decomposition of $CH_3NH_3PbI_3$, or $MAPbI_3$, can react severely with Ag and Al.

$$CH_3NH_3PbI_3 \leftrightarrow CH_3NH_2 + HI + PbI_2 \quad (1)$$

In contrast, copper (Cu) is well-known for its better corrosion resistance, especially in non-oxidizing acids (*e.g.* HI, HBr) and halogens.[34] For example, Cu can improve the resistance of a metal alloy to Cl^--rich seawater, and enhances the resistance of Cu alloys to environments containing HF.[34] The performance of Cu and its alloys in these conditions inspired us to evaluate whether Cu can be a stable electrode for halide perovskites. Here, we found that Cu may be a promising electrode material that is intrinsically stable with OIHP over long times. The accelerated degradation study revealed that in the absence of oxygen and moisture, *i.e.*, in encapsulated perovskite solar cells, Cu can be stable even in direct contact with perovskite for many years. The diffusion of Cu was not observed in perovskite after long-term thermal annealing or sun illumination. High performance device with Cu electrode can be stable for hundreds of hours in ambient environment without any encapsulation.

Results and discussion

Cu was first introduced into perovskite solar cells as an electrode by us in devices produced by the doctor-blade method, which resulted in a long device lifetime of over one month for non-encapsulated devices.[35] In the Cu/$MAPbI_3$ interface, the Cu was in direct contact with $MAPbI_3$ and has been shown to be much more stable than Al/$MAPbI_3$ and Ag/$MAPbI_3$ interfaces after one day in air, but notable reaction of Cu with $MAPbI_3$ could be observed after one week of storage in air. It is noted that Cu can still be oxidized in the presence of oxygen and moisture, and the possible oxidation products (*e.g.* $Cu(OH)_2$ or CuO_x by the reactions (2) and (3) below) can react with the decomposition products of perovskites (*e.g.* HI), which may cause perovskite decomposition by driving the reaction towards the right side (eqn (1)).[34,36]

$$Cu + H_2O + \frac{1}{2}O_2 \rightarrow Cu(OH)_2 \quad (2)$$

$$Cu + O_2 \rightarrow CuO_x \quad (3)$$

Removing oxygen and moisture, for example by encapsulation, should eliminate the oxidation and stabilize the Cu/$MAPbI_3$ interface. This was tested by annealing the samples with a structure of ITO/poly[bis(4-phenyl)(2,4,6-trimethylphenyl)amine] (PTAA)/$MAPbI_3$/Cu (Fig. 1a) at 100 °C in both air and N_2. Here we tested the stability of Cu with $MAPbI_3$ by depositing Cu directly onto $MAPbI_3$ without any charge transport layer. This evaluates the intrinsic stability between these two materials, which gives the worse-case scenario if Cu diffuses through the charge transport layers (CTLs) and predicts the lower limit of stability. As shown in Fig. 1b, after the sample was annealed in air for only 1 hour, the back side of the sample underneath the Cu electrodes turned to

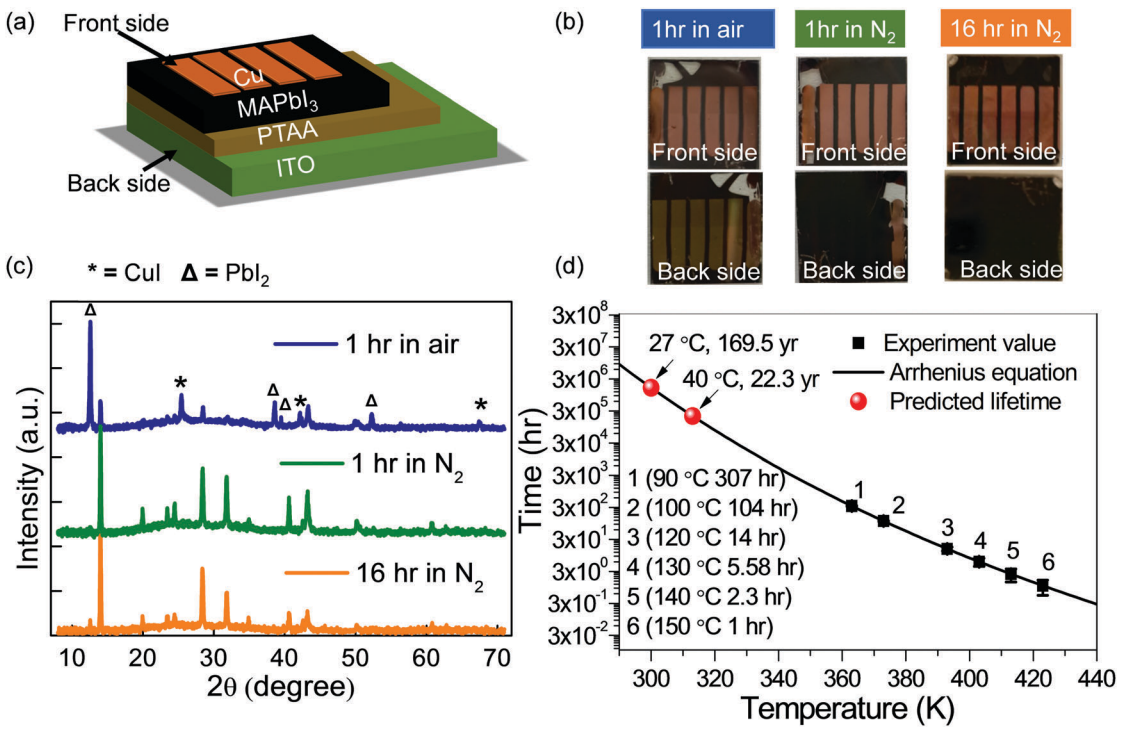

Fig. 1 (a) Diagram of the Cu/perovskite structure used for stability evaluation. (b) Photos taken from the front side and back side of the samples after being annealed at 100 °C in air and in N_2 for 1 hour and 16 hours. (c) XRD pattern of the annealed samples. (d) Measured perovskite stable time at different temperature. The black solid line shows the fitting of the experimental data with Arrhenius equation.

yellow, indicating the degradation of $MAPbI_3$ beneath the Cu electrodes and the penetration of Cu across the degraded $MAPbI_3$ layer. The corresponding X-ray diffraction (XRD) characterization of the degraded samples verified that the degradation products included CuI (its three most intense peaks are located at 25.5°, 42.2°, and 67.4° 2θ) and PbI_2 (peaks at 12.6°, 38.6°, 39.5° and 52.3° 2θ). In contrast, there was no color change for the samples annealed in an N_2 environment even after annealing for 16 hours at 100 °C. There were no peaks characteristic of CuI in the XRD spectrum, but there was a small peak associated with PbI_2, which could be caused by thermal decomposition of the perovskite film not covered by Cu (Fig. 1c). This result confirmed that the Cu/$MAPbI_3$ interface is much more stable in the absence of moisture and oxygen. It reveals the intrinsic Cu stability with $MAPbI_3$, which is meaningful and important to study, because perovskite solar cells have to be encapsulated for real applications, just like other type of thin film solar cells such as CIGS.

In order to determine the overall reaction kinetics between Cu and $MAPbI_3$ necessary to predict the lifetime of devices with Cu electrodes, annealing at elevated temperatures was done. Here the samples were covered by a thick layer of polystyrene (PS) to suppress the thermal decomposition so that the interface reaction could be studied. The stable lifetime (τ) is defined as the thermal annealing duration after which the most intense XRD peak of CuI at 25.5° 2θ appears. As shown in Fig. S1 (ESI†), the CuI XRD peaks were evident after annealing at 150 °C for 1 h, 140 °C for 2.3 h, 130 °C for 5.58 h 120 °C for 14 h, 100 °C for 104 h and 90 °C for 307 h. These points were shown time (τ) *versus* temperature (T) plot as shown in Fig. 1d, which follows a typical Arrhenius relationship.[37] From the fitting curve, the stable lifetime at lower temperature can be predicted. At room temperature (300 K), the lifetime of Cu/$MAPbI_3$ structure can be calculated to be around 1.5×10^6 hours, or 169.5 years. Even at nominal operating cell temperature of 40 °C, which is among the worst-case scenarios for poor thermal management in modules, the Cu/$MAPbI_3$ structure is still stable for more than 22 years. It should be noted that the stable lifetime might be overestimated because of the low sensitivity of XRD (typically on the order of 5% in determining phase content). While the real lifetime is less than 170 years at room temperature, in real devices there are electron/hole transport layers (*e.g.* ZnO, fullerene, NiO_x) separating the Cu and OIHP as a diffusion barrier. Nevertheless, this study still reveals that Cu is a very stable electrode for perovskite materials.

One concern of using Cu as electrode is the high diffusivity Cu in many known materials, such as porous polymers. Lattice diffusion occurs either through interstitial sites or vacancies.[38] Due to the close-packed crystal structure of OIHP with interstitial sites smaller than the radius of Cu, the interstitial diffusion of Cu in OIHP has been predicted to be slow by M. Saiful Islam *et al.*[39] For vacancy diffusion, I^- vacancies are most likely, as they were reported to have the highest concentration due to the small formation energy.[40] However, Cu with a positive charge would still have too high energy barrier to occupy the I^- vacancy site. Therefore the diffusion of Cu through OIHP is not expected to be significant. A straightforward experiment to judge whether significant Cu diffusion occurs is to deposit a very thin layer (5 nm) of Cu directly on top of $MAPbI_3$, and to observe whether Cu disappears after annealing. It was found Cu on $MAPbI_3$ remained intact even after annealing at 80 °C for 22 hours, suggesting minimal diffusion of Cu into $MAPbI_3$ (Fig. 2a). In addition, the SEM/EDX measurements were conducted to determine if Cu diffused into the $MAPbI_3$. The $MAPbI_3$ thin films were covered by a thermally-evaporated Cu layer 100 nm thick. Then the samples were annealed at 80 °C for 20 h, after which the Cu electrodes were peeled off using Kapton tape, as illustrated in Fig. 2b. One indication that little or no diffusion occurred is that the bonding between Cu and $MAPbI_3$ remained poor (*i.e.*, no diffusion bonding occurred), as the Cu can

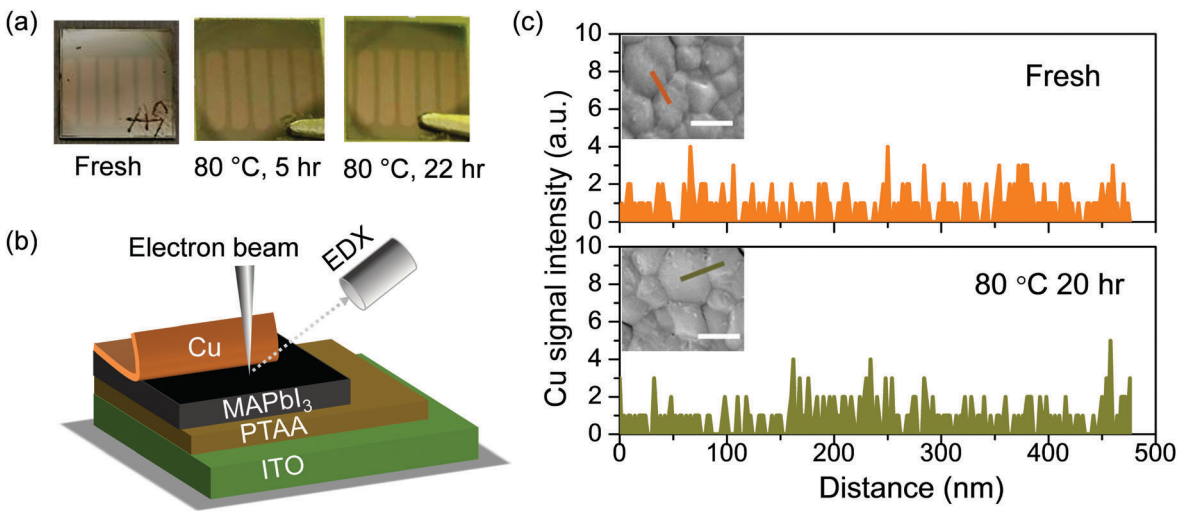

Fig. 2 (a) Photos (taken from air side) of samples with the structure of ITO/PTAA/perovskite/Cu (5 nm) before and after annealing at 80 °C for 5.0 h and 22.0 h. (b) Diagram of the sample preparation for SEM and EDX line scan. (c) The EDX line scanning of Cu signal. The scanning positions were labeled in the SEM image by the orange and green lines. The scale bar is 500 nm.

be easily peeled off. The Cu content in the $MAPbI_3$ underneath the Cu electrodes was measured before and after thermal annealing. The Cu Kα line intensity was monitored across a $MAPbI_3$ grain boundary. As shown in Fig. 2c, the Cu signal of the samples before and after annealing is indistinguishable, and the overall signal is at the level of noise. In addition, the line-scans covering both grain and grain boundaries did not show Cu intensity contrast between grain and grain boundary areas, suggesting that Cu diffusion is also negligible along grain boundary.

The possible diffusion of Cu into $MAPbI_3$ was also evaluated by monitoring the variation of the vertical electrical resistance of the ITO/PTAA/perovskite/Cu after annealing. The electrical resistance change of the devices was monitored with time under annealing at 80 °C. The thickness of the $MAPbI_3$ layer was about 360 nm (ESI,† Fig. S2). If Cu can diffuse into perovskite or along the grain boundaries during annealing, the device resistance should decrease dramatically. It should be noted that we did observe some shunted devices right after the evaporation of Cu with such a device structure without charge transport layers, though there were good working devices without shunting. The shunting observed before annealing was most likely caused by pin-holes in the polycrystalline $MAPbI_3$ films which were filled by the conductive Cu rather than by Cu diffusion through lattice or grain boundary of the perovskite film. This was verified by Conductive-Atomic Force Microscope (C-AFM). The topography of the three samples was shown in Fig. 3a–c. The first sample was a $MAPbI_3$ film without Cu. The second and third samples were the shunted and working devices, but the Cu electrodes were peeled off. As illustrated in Fig. 3d–f, the current stayed in the picoampere (pA) scale before and after annealing, and the current at the grain boundaries is even lower than that on grains for all the three samples, indicating the lack of high-conductivity Cu pathways in the sample, and thus minimal Cu diffusion. This result also indicates one main function of charge transport layers is to block the pin-holes of the polycrystalline films to increase the device open circuit voltage (V_{oc}) and fill factors (FF) due to the reduced leakage.[41] The samples without pin-holes had a resistance on the order of 10^6 ohm, which was chosen for the subsequent annealing study.

Fig. 4a shows the statistic resistance change of the working samples annealed at 80 °C. There was no obvious resistance change for the working devices even after annealing for 112.5 h, suggesting that the Cu/perovskite interface is stable under the given condition and no diffusion occurred. Despite the lack of Cu diffusion and reaction with $MAPbI_3$, it is important to understand the influence of Cu on the electronic properties of $MAPbI_3$. This study is necessary because the possibility of subtle reactions of Cu with $MAPbI_3$, which cannot be observed through material structure characterization but may cause dramatic changes in the electronic properties. Since the OIHP materials are mostly intrinsic semiconductors, only a few ppm of doping could increase the conductivity by several orders of magnitude, while possible reactions may also introduce defects and charge traps. Thus, the photovoltaic performance of the above devices was studied under thermal/light aging. We noticed that such devices without an electron transport layer also had decent photovoltaic performance under one sun illumination.

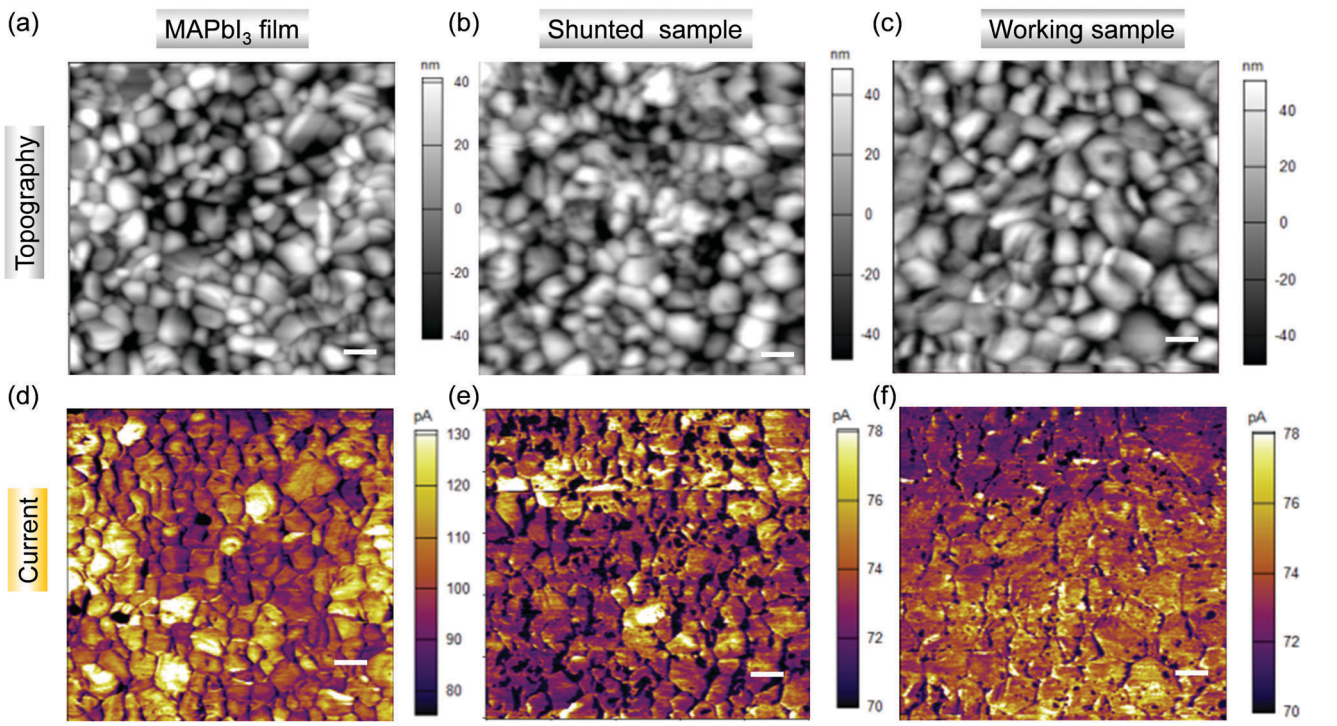

Fig. 3 (a–c) Topography and (d–f) current of the $MAPbI_3$ film, shunted sample and working sample, respectively. The scanning area for both topography and current is 5 × 5 μm^2. The scale bar is 500 nm.

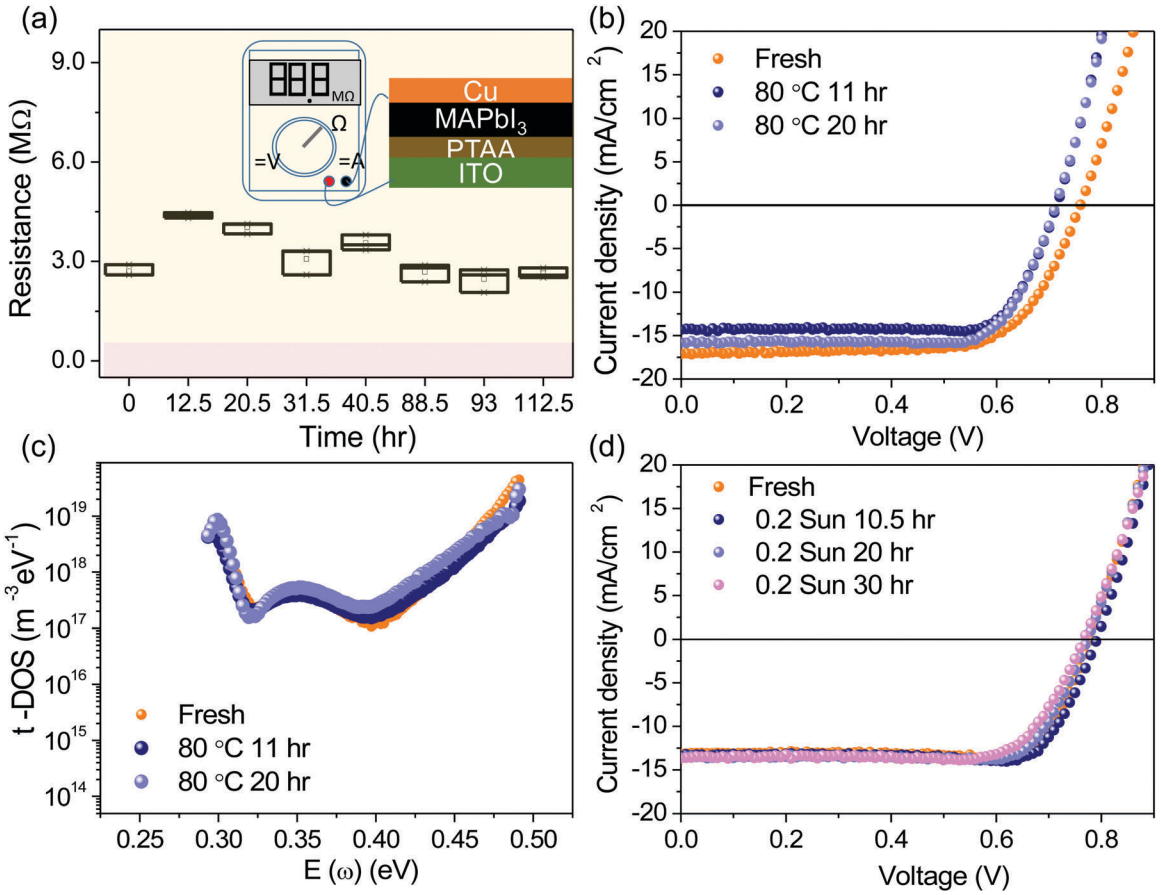

Fig. 4 (a) Electrical resistance of working sample dependence on annealing time at 80 °C. The inset is the diagram of the resistance measurement of the Cu/perovskite structure. (b) *I–V* curve and (c) the trap states of the device before and after annealing at 80 °C for 11 hours and 20 hours. (d) *I–V* curve of the device before and after 0.2 sun illumination for 30 hours.

As shown by the current–voltage (*J–V*) curve in Fig. 4b, the devices exhibited a power conversion efficiency (PCE) of 9.0% by reverse scanning before thermal annealing. After annealing at 80 °C for 20 hours, the PCE dropped slightly to 8.7%, which showed much higher stability comparing to the device with Au as electrode in a recent literature using similar accelerated aging test (75 °C for 15 hours).[33] The trap density of the device was also measured before and after thermal annealing. As shown in Fig. 4c, there was no obvious change of the trap density for the samples annealed at 80 °C for 20 hours. It suggests that Cu does not introduce extra charge trap states to the perovskite during thermal annealing process, which is in agreement with the absence of chemical reaction between Cu and $MAPbI_3$. In addition to good thermal stability, the device with such a simple structure also displayed stable performance under continuous illumination as shown in Fig. 4d. After being illuminated at light intensity of 20 mW cm^{-2} for 30 hours, the efficiency of the device only slightly decreased from 8.7% to 7.9%, which shows much slower degradation comparing to devices using other metals such as Au, Ag, Al, or Ca reported recently.[27]

Cu can also be the stable electrode for highly efficient perovskite solar cells when an ETL is inserted between the perovskite layer and Cu. The power conversion efficiency in our optimized devices reached over 20.0% when fullerene (C_{60}) and bathocuproine (BCP) as electron transport layer was inserted, and the perovskite layer was well passivated (Fig. 5a). The device efficiency *versus* storage time is shown in Fig. 5b. After 816 hours storage in air (25 °C, ~55% relative humidity) without encapsulation, the device retained 98% of the initial efficiency. The three parameters of fill factor, open circuit voltage and short circuited current almost didn't change. In comparison, the perovskite devices with Ag or Al electrodes lost 20% or more of the initial efficiency after 200 hours storage in air (25 °C, 35% humidity).[42] This clearly showed the much better stability of the perovskite solar cells with Cu electrodes.

Conclusion

In conclusion, we revealed that Cu could be an extraordinarily stable electrode material for OIHP solar cells. The chemical reaction between Cu and perovskite under inert atmosphere takes over 169 years at room temperature, and there is no notable diffusion of Cu into the perovskite. A simple device with Cu/perovskite contact can be stable under high temperature

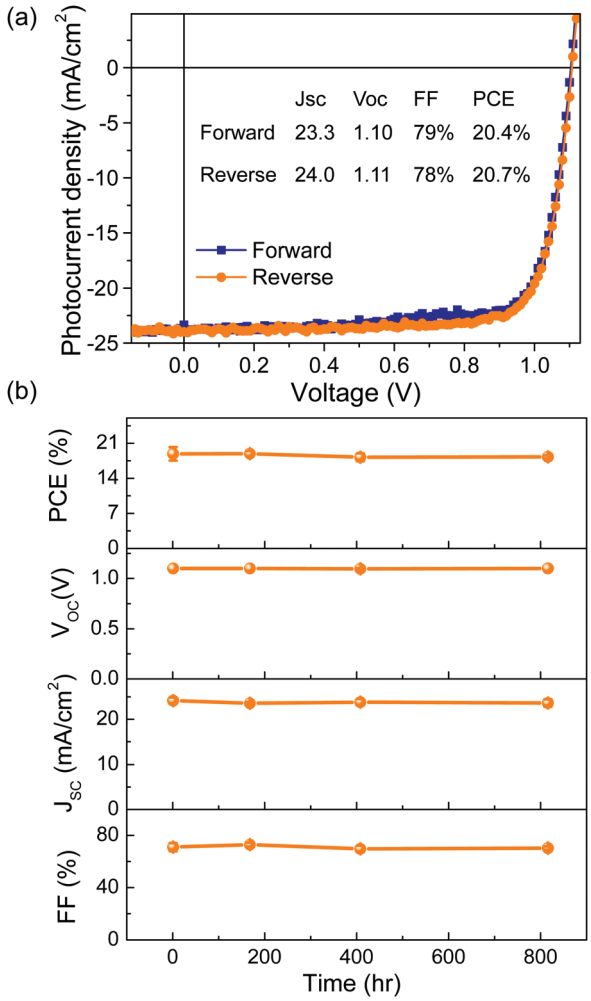

Fig. 5 (a) *J*–*V* curve of the device with electron transport layer C_{60}/BCP. (b) Device performance as a function of storage time at ambient environment condition (~55% humidity, T = 25 °C) without encapsulation.

annealing for over 100 hours. The absence of any chemical reaction between Cu and $MAPbI_3$ allows the charge trap states to remain constant under continuous annealing or illumination. For high efficiency perovskite solar cells (PCE > 20%) with Cu electrode, the efficiency sustained 98% of the initial value after over 800 hours storage in ambient environment (25 °C, ~55% humidity). Considering its high conductivity, low-cost, and high stability, Cu is a better choice for the electrode material in perovskite solar cells than other widely used electrode materials (Ag, Al, Cr or Au). Further study is still needed in order to fully understand the stability limit of perovskite solar cells, while the electrode stability is shown not to be the limiting factor here. The commercial availability of Cu ink or Cu paste also allows the scalable manufacturing of perovskite solar cells with Cu electrodes.

Methods

Perovskite thin film device fabrication

The hole transport layer, poly[bis(4-phenyl)(2,4,6-trimethylphenyl)-amine] (PTAA) film was prepared by spin-coating 2 mg mL^{-1} PTAA/toluene solution onto a clean ITO film at 4000 revolutions per minute (rpm) for 30 s. The as-prepared film was then annealed at 100 °C for 10 min. The perovskite films were fabricated on the as-prepared PTAA/ITO substrates by inter-diffusion method as is reported previously.[19] After that, an 80 nm thick Cu electrode was deposited by thermal evaporation directly on perovskite films or after perovskite films was passivated and C_{60}/BCP as electron transport layer was inserted.

X-ray diffraction (XRD)

XRD measurements were performed with the Bruker-AXS D8 Discover Diffractometer. Bruker D8 Discover diffractometer is configured in parallel beam geometry with Cu Kα radiation (wavelength of 1.5418 Å).

Energy-dispersive X-ray spectroscopy (EDS)

EDX line scan was carried out on a FEI Helios NanoLab™ 660 instrument equipped with TEAM energy dispersive spectroscope. The typical electron acceleration voltage for X-ray excitation was 15 kV. The typical acceleration current was 100 pA.

Conductive atomic force microscope

C-AFM was measured by a commercial AFM system (MFP-3D, Asylum Research, USA) and Pt/Ir coated conductive probes (PPP-EFM, Nanosensors, Switzerland). The topography and surface current were measured by C-AFM in the dark and in N_2. DC bias applied here is 1 V. The schematic diagram is shown in Fig. 4b. Samples for C-AFM characterization were also the devices with Cu electrodes being peeled off by Kapton tape.

Electrical characterization

During all electrical characterization, perovskite devices were kept in a N_2 glovebox to protect the samples. The *J*–*V* performance of the samples was recorded using a Keithley 2400 semiconductor analyzer. The scanning rate is 0.1 V s^{-1}. Simulated AM 1.5 G irradiation (100 mW cm^{-2}) was produced by a xenon-lamp-based solar simulator (Oriel 67005, 150 W Solar Simulator) for current (*I*)–voltage (*V*) measurements. The light intensity was calibrated by a silicon (Si) diode (Hamamatsu S1133) equipped with a Schott visible colour glass filter (KG5 color filter).

Acknowledgements

This work was supported by the National Science Foundation (DMR-1505535), Department of Energy (DE-EE0006709), and Office of Naval Research (N00014-15-1-2713). The research was performed in part in the Nebraska Nanoscale Facility: National Nanotechnology Coordinated Infrastructure, the Nano-engineering Research Core Facility, and the Nebraska Center for Materials and Nanoscience, which are supported by the National Science Foundation under Award ECCS: 1542182, and the Nebraska Research Initiative.

References

1 J. Gong, S. B. Darling and F. You, *Energy Environ. Sci.*, 2015, **8**, 1953–1968.
2 M. Liu, M. B. Johnston and H. J. Snaith, *Nature*, 2013, **501**, 395–398.
3 M. A. Green, A. Ho-Baillie and H. J. Snaith, *Nat. Photonics*, 2014, **8**, 506–514.
4 J. Burschka, N. Pellet, S.-J. Moon, R. Humphry-Baker, P. Gao, M. K. Nazeeruddin and M. Grätzel, *Nature*, 2013, **499**, 316–319.
5 H. Zhou, Q. Chen, G. Li, S. Luo, T.-b. Song, H.-S. Duan, Z. Hong, J. You, Y. Liu and Y. Yang, *Science*, 2014, **345**, 542–546.
6 M. D. McGehee, *Nat. Mater.*, 2014, **13**, 845–846.
7 J. H. Heo, S. H. Im, J. H. Noh, T. N. Mandal, C.-S. Lim, J. A. Chang, Y. H. Lee, H.-j. Kim, A. Sarkar and M. K. Nazeeruddin, *Nat. Photonics*, 2013, **7**, 486–491.
8 M. M. Lee, J. Teuscher, T. Miyasaka, T. N. Murakami and H. J. Snaith, *Science*, 2012, **338**, 643–647.
9 W. Nie, H. Tsai, R. Asadpour, J.-C. Blancon, A. J. Neukirch, G. Gupta, J. J. Crochet, M. Chhowalla, S. Tretiak and M. A. Alam, *Science*, 2015, **347**, 522–525.
10 K. Hwang, Y. S. Jung, Y. J. Heo, F. H. Scholes, S. E. Watkins, J. Subbiah, D. J. Jones, D. Y. Kim and D. Vak, *Adv. Mater.*, 2015, **27**, 1241–1247.
11 L. Gouda, R. Gottesman, S. Tirosh, E. Haltzi, J. Hu, A. Ginsburg, D. A. Keller, Y. Bouhadana and A. Zaban, *Nanoscale*, 2016, **8**, 6386–6392.
12 W. Chen, Y. Wu, Y. Yue, J. Liu, W. Zhang, X. Yang, H. Chen, E. Bi, I. Ashraful and M. Grätzel, *Science*, 2015, **350**, 944–948.
13 Y. Zhou, M. Yang, O. S. Game, W. Wu, J. Kwun, M. A. Strauss, Y. Yan, J. Huang, K. Zhu and N. P. Padture, *ACS Appl. Mater. Interfaces*, 2016, **8**, 2232–2237.
14 J. Huang, Y. Shao and Q. Dong, *J. Phys. Lett.*, 2015, **6**, 3218–3227.
15 M. Hu, C. Bi, Y. Yuan, Y. Bai and J. Huang, *Adv. Sci.*, 2015, **3**, 1500301.
16 N. J. Jeon, J. H. Noh, W. S. Yang, Y. C. Kim, S. Ryu, J. Seo and S. I. Seok, *Nature*, 2015, **517**, 476–480.
17 W. S. Yang, J. H. Noh, N. J. Jeon, Y. C. Kim, S. Ryu, J. Seo and S. I. Seok, *Science*, 2015, **348**, 1234–1237.
18 B. J. Kim, D. H. Kim, Y.-Y. Lee, H.-W. Shin, G. S. Han, J. S. Hong, K. Mahmood, T. K. Ahn, Y.-C. Joo and K. S. Hong, *Energy Environ. Sci.*, 2015, **8**, 916–921.
19 C. Bi, Q. Wang, Y. Shao, Y. Yuan, Z. Xiao and J. Huang, *Nat. Commun.*, 2015, **6**, 7747.
20 NREL Best Research-Cell Photovoltaic Efficiency Chart, https://upload.wikimedia.org/wikipedia/commons/archive/3/35/20160317201049%21Best_Research-Cell_Efficiencies.png.
21 X. Li, D. Bi, C. Yi, J.-D. Décoppet, J. Luo, S. M. Zakeeruddin, A. Hagfeldt and M. Grätzel, *Science*, 2016, aaf8060.
22 G. Niu, X. Guo and L. Wang, *J. Mater. Chem. A*, 2015, **3**, 8970–8980.
23 Y. Yuan and J. Huang, *Acc. Chem. Res.*, 2016, **49**, 286–293.
24 D. Bryant, N. Aristidou, S. Pont, I. Sanchez-Molina, T. Chotchunangatchaval, S. Wheeler, J. R. Durrant and S. A. Haque, *Energy Environ. Sci.*, 2016, **9**, 1655–1660.
25 Y. Han, S. Meyer, Y. Dkhissi, K. Weber, J. M. Pringle, U. Bach, L. Spiccia and Y.-B. Cheng, *J. Mater. Chem. A*, 2015, **3**, 8139–8147.
26 Y. Kato, L. K. Ono, M. V. Lee, S. Wang, S. R. Raga and Y. Qi, *Adv. Mater. Interfaces*, 2015, **2**, 1500159.
27 A. Guerrero, J. You, C. Aranda, Y. S. Kang, G. Garcia-Belmonte, H. Zhou, J. Bisquert and Y. Yang, *ACS Nano*, 2015, **10**, 218–224.
28 J. H. Park, J. Seo, S. Park, S. S. Shin, Y. C. Kim, N. J. Jeon, H. W. Shin, T. K. Ahn, J. H. Noh and S. C. Yoon, *Adv. Mater.*, 2015, **27**, 4013–4019.
29 M. Kaltenbrunner, G. Adam, E. D. Głowacki, M. Drack, R. Schwödiauer, L. Leonat, D. H. Apaydin, H. Groiss, M. C. Scharber and M. S. White, *Nat. Mater.*, 2015, **14**, 1032–1039.
30 J. You, L. Meng, T.-B. Song, T.-F. Guo, Y. M. Yang, W.-H. Chang, Z. Hong, H. Chen, H. Zhou and Q. Chen, *Nat. Nanotechnol.*, 2016, **11**, 75–81.
31 E. M. Sanehira, B. J. Tremolet de Villers, P. Schulz, M. O. Reese, S. Ferrere, K. Zhu, L. Y. Lin, J. J. Berry and J. M. Luther, *ACS Energy Lett.*, 2016, **1**, 38–45.
32 W. Chen, Y. Wu, J. Liu, C. Qin, X. Yang, A. Islam, Y.-B. Cheng and L. Han, *Energy Environ. Sci.*, 2015, **8**, 629–640.
33 K. Domanski, J.-P. Correa-Baena, N. Mine, M. K. Nazeeruddin, A. Abate, M. Saliba, W. Tress, A. Hagfeldt and M. Grätzel, *ACS Nano*, 2016, **10**, 6306–6314.
34 R. W. Revie, *Corrosion and corrosion control*, John Wiley & Sons, 2008.
35 Y. Deng, Q. Dong, C. Bi, Y. Yuan and J. Huang, *Adv. Energy Mater.*, 2016, **6**, 1600372.
36 J. S. Manser, M. I. Saidaminov, J. A. Christians, O. M. Bakr and P. V. Kamat, *Acc. Chem. Res.*, 2016, **49**, 330–338.
37 S. Schuller, P. Schilinsky, J. Hauch and C. Brabec, *Appl. Phys. A: Mater. Sci. Process.*, 2004, **79**, 37–40.
38 R. W. Balluffi, S. Allen and W. C. Carter, *Kinetics of Materials*, John Wiley & Sons, 2005.
39 C. Eames, J. M. Frost, P. R. Barnes, B. C. O'regan, A. Walsh and M. S. Islam, *Nat. Commun.*, 2015, **6**, 7497.
40 D. Yang, W. Ming, H. Shi, L. Zhang and M.-H. Du, *Chem. Mater.*, 2016, **28**, 4349–4357.
41 Q. Wang, Y. Shao, Q. Dong, Z. Xiao, Y. Yuan and J. Huang, *Energy Environ. Sci.*, 2014, **7**, 2359–2365.
42 H. Back, G. Kim, J. Kim, J. Kong, T. K. Kim, H. Kang, H. Kim, J. Lee, S. Lee and K. Lee, *Energy Environ. Sci.*, 2016, **9**, 1258–1263.

